A multirate approach to combine electromagnetic transients and fundamental-frequency simulations

F. Plumier, C. Geuzaine, and T. Van Cutsem

Abstract—A new multi-rate technique is proposed to combine fundamental-frequency simulation (typical of stability studies) with electromagnetic transients simulation. The objective of this hybrid approach is to obtain more accurate simulations than with the fundamental-frequency approximation, while saving computing time by applying the detailed model to a subsystem only, in some neighbourhood of the disturbance. It also allows to remove some limitations of fundamental-frequency simulation, such as the difficulty of simulating unbalanced faults. A relaxation technique is used to iterate between both models with simple interfacing. Preliminary results obtained with a 74-bus test system are presented, together with a comparison with full electromagnetic transients simulation.

Keywords—Power system dynamics, electromagnetic transients, fundamental-frequency approximation, multirate simulation.

I. Introduction

Traditional power system modeling and simulation techniques can be grouped into two families [1]: (i) Electro-Magnetic Transient (EMT) simulations focus on small time constant phenomena, typically from milliseconds to hundreds of milliseconds; (ii) Fundamental-Frequency (FF) approximation, also referred to as quasi-sinusoidal, or phasor-mode or Transient Stability approximation covers slower phenomena, such as electromechanical oscillations, load restoration, or thermodynamical processes. It ranges typically from hundreds of milliseconds to hundreds of seconds.

However, each of these models has its limitations. Since FF typically relies on positive-sequence representation, simulation of unbalanced faults is not easy and cannot account for distortions of the FF sine wave (such as aperiodic components, harmonics, etc.). EMT simulations, on the other hand, are much more accurate but also time-consuming, which makes them inappropriate to deal with large-scale systems.

Alternative modeling approaches were proposed to overcome the disadvantages of each method while trying to keep its advantages. For instance, the dynamic phasor modeling retains in the dynamic response a few terms of Fourier series with varying amplitudes and phase angles [2]. However, this approach requires to determine the number of terms to be kept in the model in order to correctly represent the phenomena of interest. Another recent approach is the frequency-adaptive simulation of transients which aims at representing both electromagnetic and electromechanical transients within a single tool [3], [4].

Instead of developing new models, it may be attractive to combine the existing, proven and much used by industry, EMT and FF simulations. This led to the development of hybrid simulation combining both models. Such approaches can be traced back to the pioneering work in [5], [6]. Since then, many improvements were brought to the initial method regarding interface location, extraction method, equivalencing one subsystem in the other, etc. Recently, some authors also applied the method to asymmetrical faults [7] and Voltage Source Converter High-Voltage DC links [8]. A detailed literature review is available in [1].

To the best knowledge of the authors, most hybrid simulation methods proposed so far rely on direct (either series or parallel) schemes that do not iterate between the FF and EMT models at a given time step. However, some limitations inherent to a non-iterative approach are shown in [9]. In particular, the use of a predefined equivalent impedance kept constant from the beginning till the end of the simulation is shown to give wrong results in some cases. On the contrary, the method proposed in this paper uses a relaxation scheme inspired of multi-rate simulation methods. In this spirit, the FF model is simulated with a "large" step H while the EMT model is integrated with successive "small" steps h over the same time interval H. Iterations between both models take place until the respective simulations match at the end of the large step H. Compared to direct hybrid simulation, this approach does not require replacing the sub-domain treated in FF simulation by an equivalent when dealing with the sub-domain treated in EMT simulation, and ensures proper synchronization between the FF and EMT simulations.

II. Multirate hybrid simulation method

A. Overview of the method

The power system is decomposed into several sub-domains. Every line of the system is included into one and only one sub-domain. The boundary between sub-domains is constituted of the busbars. A decomposition into two sub-domains is sketched in Fig. 2.

We outline the multirate procedure used to simulate the system evolution from t to $t + H$ (a typical value for H is one cycle at fundamental frequency, i.e. 20 or 16.67 ms). The relaxation scheme is outlined in Fig. 1. The procedure starts with the integration of the differential-algebraic equations of the FF model. At time $t + H$, interface variables are passed
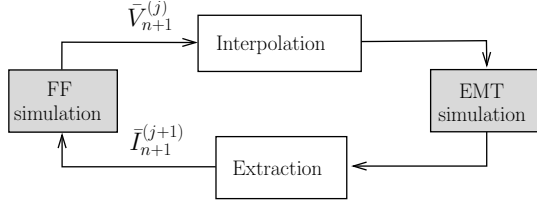
Figure 1. Principle of the relaxation scheme: Gauss-Seidel relaxation until convergence. The subscript indicates the time-step being computed while the superscript refers to the iteration number to compute this particular time step.
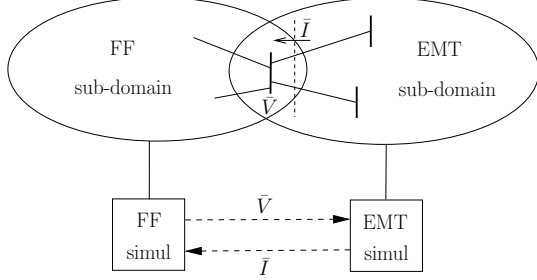

Figure 2. FF and EMT sub-domains and exchanged variables between FF and EMT simulations (case of one boundary bus).

Figure 3. EMT and FF step sizes.

from the FF to the EMT sub-domain. Then, the differential-algebraic equations of the EMT model are integrated over $[t, t+H]$ with the small step h (typical value: $100\,\mu s$) using at each discretized time interpolated values of the interface variables stemming from the FF sub-domain. At time $t+H$ other interface values are passed back from the EMT to the FF sub-domain. Using these values, a new integration of the FF model is performed from t to $t+H$. The procedure is repeated until a convergence test is satisfied at $t+H$.

Each sub-domain being solved with the last values of the interface variables relative to the other sub-domain, the relaxation scheme is of the Gauss-Seidel type. This requires the FF and EMT simulations to be performed sequentially (unlike most of the direct methods mentioned in the Introduction). With the proper computer hardware, the FF and the EMT simulations over each time interval of duration H could be run in parallel, using a Gauss-Jacobi relaxation scheme [10] but the Gauss-Seidel scheme is known to have better convergence. Parallel computation is no further considered in this paper.

B. Exchanged interface variables

Regarding interface variables, it was found convenient to pass bus voltages from the FF to the EMT simulation, and currents injected into buses from the EMT to the FF simulation as sketched in Fig. 2. An alternative would consist of exchanging active and reactive powers, but this can be problematic in the (uncommon) case of very low voltage at the interface between sub-domains. Passing currents to the FF simulation is convenient in so far as the latter usually relies on current equations (in rectangular coordinates) derived from the nodal admittance matrix to describe the network part of the model.

C. Interface location

When simulating a large disturbance, such as a fault, the event is supposed to take place in the EMT sub-domain,
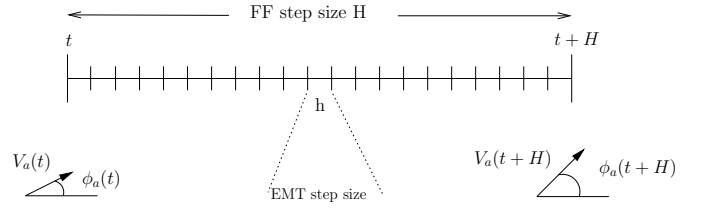
for accuracy reasons. The choice of the sub-domain interface results from the following compromise. On one hand, the EMT sub-domain should be as small as possible (for computational efficiency). On the other hand, the boundary should be far enough from the disturbance so that the harmonic contents, the DC components and the phase imbalance are kept small, to be compatible with the FF approximation. This important aspect of the coupling will be illustrated in the results section.

D. Interpolation

At each interface bus, the voltage, at time $t+H$, received from the FF simulation (that relies on positive-sequence representation) is first converted from single-phase to three-phase. Then, the amplitudes and phase angles of each phase voltage are linearly interpolated over the $[t, t+H]$ interval, as sketched on Fig. 3 where H has been considered a multiple of h, for simplicity. Considering phase a, for instance, the voltage evolution is taken as ($k = 0, 1, 2, \ldots, k_{max} = \frac{H}{h}$):

$$v_a(t+kh) = \\ \sqrt{2}\, V_a(t+kh)\, \sin\left(\omega(t+kh) + \phi_a(t+kh)\right) \quad \text{(1a)}$$

where $V_a(t+kh) =$

$$V_a(t) + [V_a(t+H) - V_a(t)] \cdot \frac{k}{k_{max}} \quad \text{(1b)}$$

and $\phi_a(t+kh) =$

$$\phi_a(t) + [\phi_a(t+H) - \phi_a(t)] \cdot \frac{k}{k_{max}} \quad \text{(1c)}$$

where ω is the nominal angular speed of the system.

In case of a major event such as a short-circuit at the beginning t of a time window $[t, t+H]$, the assumption of linear evolution of V_a and ϕ_a over $[t, t+H]$ is not valid any longer. In this case, it is recommended to make a smaller step $H' < H$ in FF simulation to absorb the effect of the event, before proceeding with the prevailing step H. This is likely to provide more accurate results than the technique presented in [9], which consists of using the values calculated at $t+H$ for the voltage magnitude and phase angle.

E. Extraction

The extraction process consists of processing the three-phase currents at the boundary of the detailed sub-domain and converting them into a single current phasor to be processed by the FF simulation. Ideally, this extraction process should not introduce delay between the variables of the detailed model and the extracted phasor. Another important point of
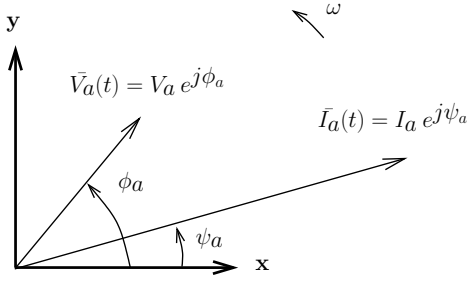
Figure 4. xy-axes used for computation of amplitude and phase angle of the positive-sequence component of the currents at the boundary.

this extraction process is the handling of discontinuities in the simulation such as fault application or clearing.

Since the first works on hybrid simulation, various extraction techniques have been contemplated. Turner et al. [6] used RMS values of the instantaneous power:

$$P_{RMS} = \frac{1}{N} \sum_{n=1}^{N} v_N i_N \qquad (2)$$

where N is the number of samples over a period of the voltage evolution and v_N and i_N are respectively the voltage and current samples.

This technique was used to avoid having to compute the Fast Fourier Transform (FFT) of the currents at the boundary. Reeve and Adapa [11] used least-squares curve-fitting for all three phases to extract the fundamental amplitude and phase angle from the sequence of simulated points, from which the positive sequence is computed. On the other hand, more recently, some authors have used FFT to extract the fundamental frequency component of the signals [9].

In the work reported here, the amplitude and phase angle of the positive-sequence component of the currents are computed from the three time-varying current waveforms, by projecting them on reference (x, y) axes, according to a transform of the Park type. The axes, sketched in Fig. 4, are orthogonal, rotate at the nominal angular speed ω and are used in FF simulation to refer all phasors to a common reference. Thus, with respect to a fixed reference, the x-axis is at an angular position:

$$\theta = \omega t + \theta_0 = \omega t \qquad (3)$$

where the position of the x-axis at $t = 0$ was arbitrarily set to $\theta(t = 0) = \theta_0 = 0$.

This technique, much used in converter Phase Locked Loop (PLL) systems [12], is free from any delay between EMT and FF simulations, provided that the applied digital post-filtering, if any, is also delay-free.

The currents take on the form:

$$\mathbf{i}_{abc} = \begin{bmatrix} i_a \\ i_b \\ i_c \end{bmatrix} = \begin{bmatrix} \sqrt{2} I_a \cos(\omega t + \psi_a) + \epsilon_a \\ \sqrt{2} I_a \cos\left(\omega t + \psi_a - \frac{2\pi}{3}\right) + \epsilon_b \\ \sqrt{2} I_a \cos\left(\omega t + \psi_a - \frac{4\pi}{3}\right) + \epsilon_c \end{bmatrix} \qquad (4)$$

where ϵ_a, ϵ_b and ϵ_c represent deviations from the perfect situation of sinusoidal positive-sequence components. They are

projected on the above mentioned axes by applying the linear transform [13]:

$$\mathbf{i}_{0xy} = \mathbf{T} \mathbf{i}_{abc} \qquad (5)$$

where

$$\mathbf{T} = \frac{\sqrt{2}}{3} \begin{bmatrix} 1/\sqrt{2} & 1/\sqrt{2} & 1/\sqrt{2} \\ \cos(\theta) & \cos\left(\theta - \frac{2\pi}{3}\right) & \cos\left(\theta - \frac{4\pi}{3}\right) \\ -\sin(\theta) & -\sin\left(\theta - \frac{2\pi}{3}\right) & -\sin\left(\theta - \frac{4\pi}{3}\right) \end{bmatrix} \qquad (6)$$

and $\mathbf{i}_{0xy}$ is the vector of instantaneous components.

Assuming that the signals have three-phase symmetry, one has $\epsilon_a = \epsilon_b = \epsilon_c = 0$ and the projected currents are mereby:

$$\mathbf{i}_{0xy} = \begin{bmatrix} I_0 \\ I_x \\ I_y \end{bmatrix} = \begin{bmatrix} 0 \\ I_a \cos \psi_a \\ I_a \sin \psi_a \end{bmatrix} \qquad (7)$$

The sought single-phase magnitude and phase angle are then given respectively by:

$$I_a = \sqrt{I_x^2 + I_y^2} \qquad \psi_a = \arctan\left(\frac{I_y}{I_x}\right) \qquad (8)$$

Note that the above projection is only applied to the currents $\mathbf{i}_{abc}$ obtained at time $t + H$.

The values (8) of the positive-sequence are passed back to the FF simulation. Clearly, if aperiodic, negative-sequence or zero-sequence components or harmonics are present in the currents $\mathbf{i}_{abc}$, it is required to filter those components to extract the slowly varying amplitude and phase angle of the positive-sequence at the desired time instants. With such a filter, the projection (5) needs to be repeated at intermediate times in the interval $[t, t + H]$.

F. Monitoring the validity of hybrid approach

The validity of the hybrid approach can be evaluated at any time and without resorting to a benchmark simulation, by monitoring the distortion, imbalance and DC components of the three-phase currents injected at the interface. If those deviations from ideal balanced three-phase sinusoidal currents are sufficiently small, then the variables at the interface are in agreement with the FF approximation, thereby making the hybrid simulation valid. If not, the boundary should be located farther away from the disturbance location, thereby making the EMT sub-domain larger.

III. SIMULATION RESULTS

A. Test system and computing tools

Tests have been performed on the 74-bus, 102-branch, 20-machine Nordic32 test system documented in [14] and shown in Fig. 5. The RAMSES software developed at the University of Liège has been used for FF simulation [15], while the EMT sub-domain solver was implemented in MATLAB, communicating with RAMSES. The results of the multirate hybrid simulation have been compared to those of an EMTP-RV simulation of the whole system.

The step size h was set to 100 μs, while H was set to 0.02 s. The trapezoidal rule was used in both FF and MATLAB-based EMT solvers.

This paper reports on preliminary tests of the proposed method. In this context, only one small EMT sub-domain was
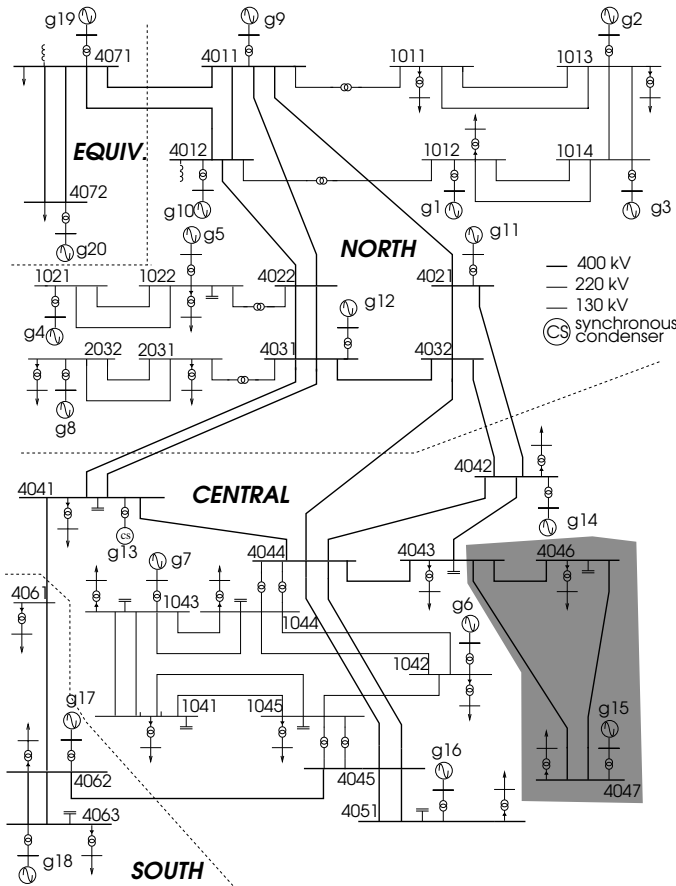
Figure 5. Nordic32 test system (EMT sub-domain shown with shade). Bus 4043 is the interface bus.

Table I
MAIN CHARACTERISTICS OF THE IMPLEMENTED MODELS.

	EMT (abc)	positive-seq. FF
Synchronous machines	2 d-axis and 2 q-axis rotor windings	Same model with transformer voltages neglected
	Simplification: Saturation ignored	
Transformers	Transformer ratio & leakage inductance	
	Simplifications: no copper losses, no saturation	
Lines	Constant pi model	
Loads	Constant impedance model	
Breakers	Open each phase at zero-crossing	No distinction between phases

B. Modeling

A comparison of the models used in FF and in EMT subsystems is presented in Table I.

The loads were modeled as constant impedances, and the lines with constant pi models for simplicity and without lack of generality. The 1200-MVA synchronous machine g15 has a constant torque, also for simplicity. More details and parameters can be found in [14].

C. Tool validation

As a preliminary step, the EMT solver implemented in MATLAB was validated, on the detailed sub-domain only, comparing its output results with those given by EMTP-RV. In this test, the remaining of the system (i.e. the non-shaded part in Fig. 5) was replaced by a constant voltage source at fundamental frequency.

A single-phase fault was assumed on line 4046-4047, near bus 4047, cleared by opening the three phases of the faulted line.

Figure 6 shows the current in phase a received by the above mentioned voltage source, before, during and after the fault. The evolutions do not show any significant difference between the MATLAB-based EMT solver and the benchmark EMTP-RV. Indeed, a much closer view of the curve is required to distinguish between the two implementations of the EMT models of the detailed sub-domain. Thus, for the level of detail expected from the hybrid FF-EMT simulation, the EMT solver can be considered equivalent to EMTP-RV.

D. Test case 1: tripping of line 4046-4047

The first test case relates to the mere tripping, at $t = 0.04$ s, of line 4046-4047 located in the EMT sub-domain. Clearly, this case is not very representative of a typical application of hybrid simulation; it was chosen for its lower severity, compatible with the already mentioned small size of the EMT sub-domain.

This case shows no negative-sequence component in the current received by the boundary bus, but a very small aperiodic component, decaying very fast. Since the three phase currents injected into the boundary bus are predominantly of the positive-sequence type, the hybrid FF-EMT simulation is expected to provide results close to those of the benchmark, since the simplifying assumptions of FF simulation are fulfilled. Figures 7, 8 and 9, relative to respectively the rotor speed of generator g15, and the boundary voltage and current, show
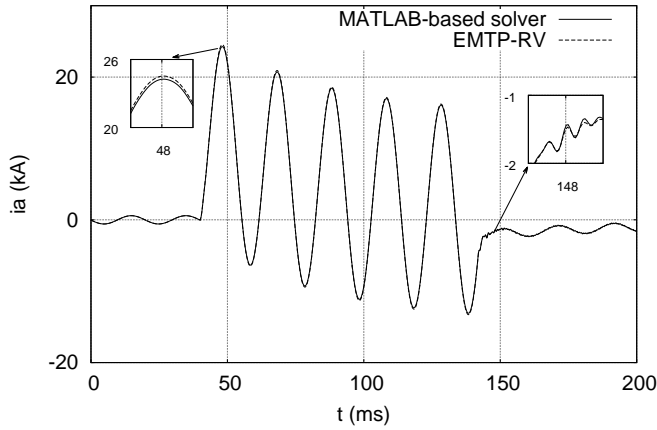
considered. It is shown with shade in Fig. 5 and includes six buses, two loads and one synchronous machine represented in detail. It is connected to the rest of the system through a single interface bus (4043 in Fig. 5).

It must be emphasized that the small size of the EMT sub-domain makes its boundary with the FF sub-domain very close to the location of disturbance, which will impact accuracy of the results for commonly considered disturbances. Due to the small size of the EMT sub-domain, we had to filter out the undesirable components of the currents injected at the boundary bus. We used a notch filter with the following transfer function:

$$H(s) = \frac{ks}{s^2 + ks + \omega_0^2} \tag{9}$$

where ω_0 is the filtered angular frequency and where the parameter k sets the sharpness of the transition between the passband and the stopbands.

For instance, to extract from I_x and I_y the components at nominal frequency (corresponding to DC components in a stationary frame), we used $k = 350$ and $\omega_0 = 2\pi 50$. We then removed these undesirable components from the original I_x and I_y to get slowly varying amplitude and phase angle as assumed for an FF simulation.

Figure 6. Current in phase a received by voltage source at bus 4043, obtained from MATLAB-based EMT solver and EMTP-RV, respectively.
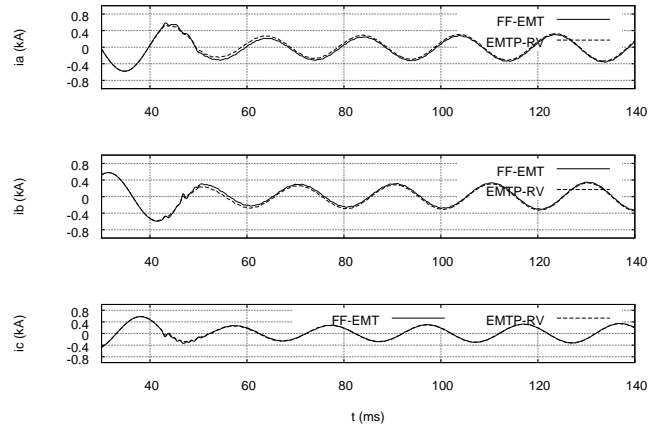

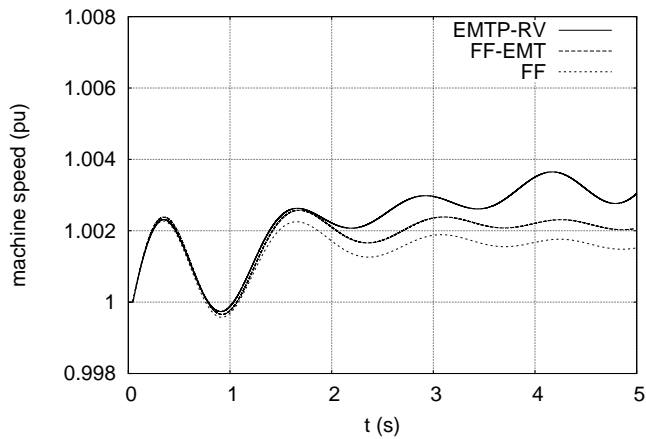Figure 9. Test Case 1: phase currents injected at boundary bus 4043

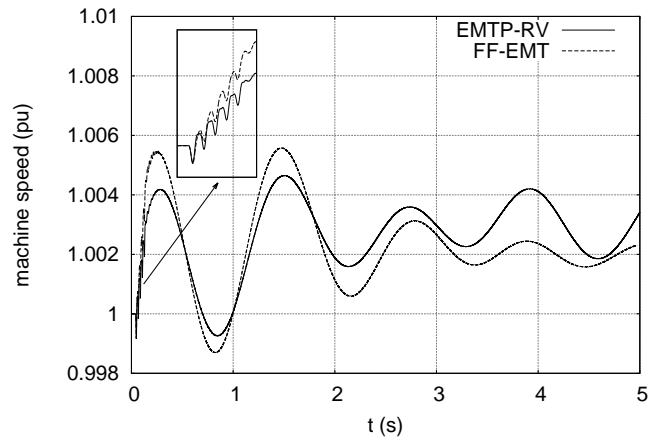Figure 7. Test Case 1: rotor speed of machine g15

Figure 10. Test Case 2: Rotor speed of machine g15

sense since the former has a full detailed and the latter full simplified model.

E. Test case 2: Single-phase fault at bus 4047

In this second test case, a single-phase solid fault is applied at $t = 0.04$ s on line 4046-4047, very near bus 4047; it is cleared by opening all three phases at $t = 0.14$ s (i.e. after 5 cycles). The rotor speed evolution of machine g15, given by EMTP-RV and FF-EMT, respectively, is shown in Fig. 10. The trajectories are close but non negligible differences are observed in this case. In fact, during the fault-on period, the machine accelerates more when simulated with FF-EMT than with EMTP-RV, indicating that a braking torque component is affected by the proximity of the FF sub-domain.

A comparison of voltage evolutions at the boundary bus 4043 is given in Fig. 11. The curve shown with solid line is the direct-sequence component of the three phase voltages computed by EMTP-RV while the dashed curve shows the corresponding voltage given by FF-EMT simulation. In fact, the currents received by the boundary bus are significantly unbalanced and have decaying DC components. However, while the positive-sequence component enters the FF simulation, the other sequence and DC components do not. The effect of the former is to make the voltage drop more significantly during
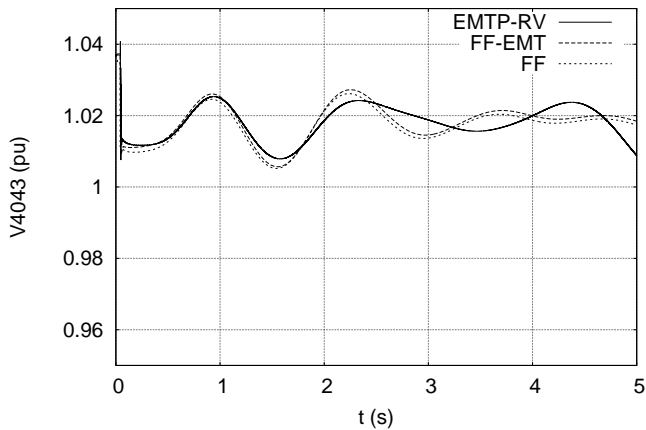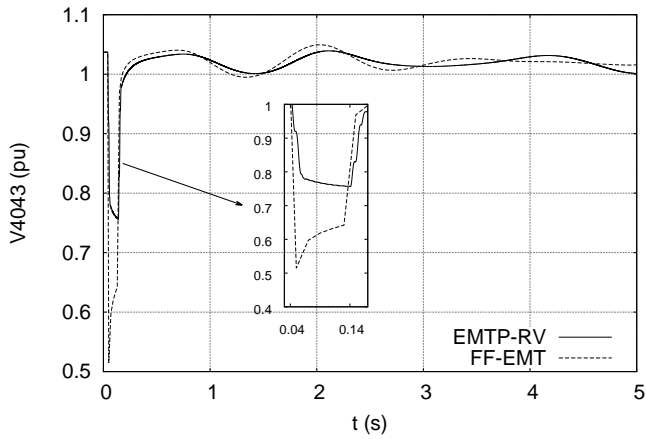

Figure 8. Test Case 1: Voltage magnitude at boundary bus 4043

indeed a good agreement between the benchmark (EMTP-RV) and the hybrid (FF-EMT) evolutions. With a larger EMT subdomain, better accuracy is to be expected.

For comparison purposes, Figs. 7 and 8 also show the response obtained with FF simulation applied to the whole system. It is noteworthy that the FF-EMT evolution fall between the EMT and the FF simulation results, which makes

Figure 11. Test Case 2: Voltage magnitude at interface bus 4043
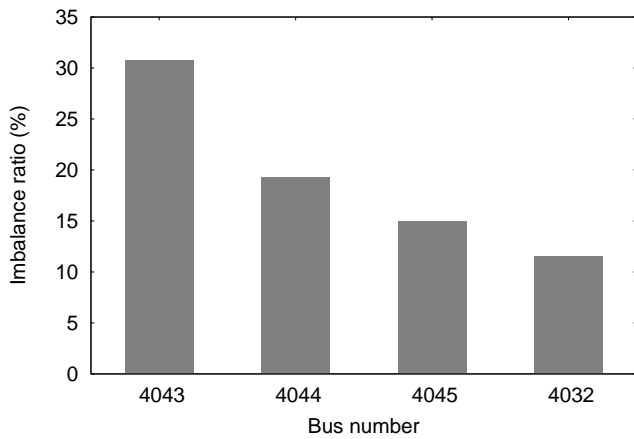
Figure 12. Test Case 2: imbalance ratio V_i/V_d at various buses

Figure 13. Test Case 3: currents received by the boundary bus 4043, obtained with EMTP-RV

Figure 14. Test Case 3: rotor speed of machine g15

Figure 15. Test Case 3: current in phase a received by the boundary bus 4043
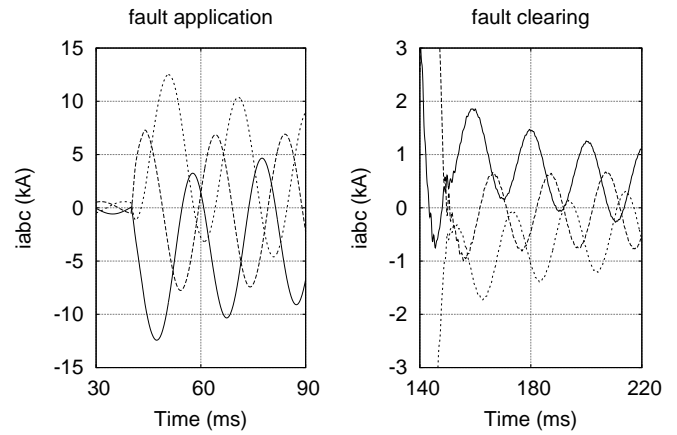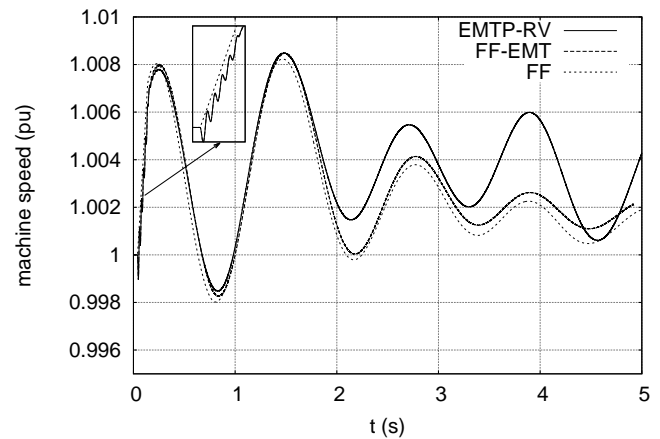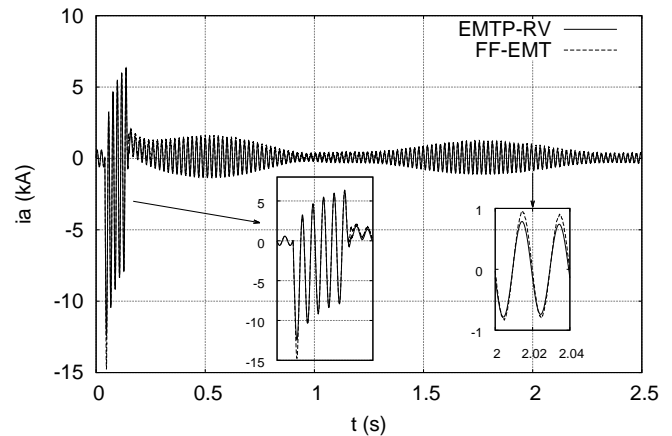
the fault, as if the FF model was subject to a three-phase fault located closer to the boundary bus.

The strong imbalance experienced in this case is confirmed by Fig. 12, showing the V_i/V_d ratio, where V_i (resp. V_d) is the magnitude of the negative (resp. positive) sequence component of the voltages at various buses. The values are averages over the fault-on period.

For better accuracy, the boundary between EMT and FF sub-domains should be moved farther away from the disturbance. How large the EMT sub-domain should be, for a given disturbance, can be assessed by observing in the FF-EMT simulation, the current imbalance ratio at the various boundary buses, shortly after the disturbance inception, and enlarging the EMT sub-domain until that ratio falls below some tolerance.

F. Test case 3: Three-phase fault at bus 4047

This last case involves a three-phase solid fault at bus 4047. It was chosen for having larger DC components compared to the previous case, as shown in Fig. 13, but negligible inverse- and zero-sequence components, relative to the currents received by the boundary bus 4043. During the fault, the DC components have initial magnitudes comparable to those of the oscillatory component.

Figures 14, 15 and 16 show respectively the rotor speed of generator g15 and the boundary current and voltage in phase a.

As already mentioned, the DC component is ignored by the FF simulation, which leads to some discrepancies. The latter, however, are of reasonable magnitude considering the small size of the EMT sub-domain. Once again, this sub-domain should be enlarged.

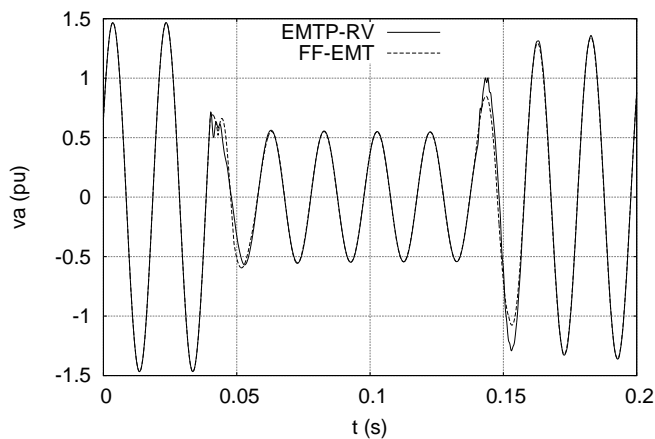As regards the rotor speed of generator g15 (see Fig. 14),

Figure 16. Test Case 3: voltage of phase a at the boundary bus 4043

in the FF simulation applied to the whole system, it increases linearly during the fault; this is to be expected since the electromagnetic torque in the FF model falls to zero during the fault, giving a constant acceleration to the rotor under the effect of the constant mechanical torque. The EMTP-RV model shows an additional oscillatory torque due to DC components of stator currents. This is also captured by the FF-EMT simulation. The discrepancy observed in Fig. 14 after $t \simeq 2$ s still needs to be clarified (it could originate from an inconsistency between EMTP-RV and FF models).

IV. Conclusion

A new method has been proposed for hybrid simulation of a detailed electromagnetic transients model combined with a fundamental-frequency model, typical of stability studies. The former is intended to be used in a sub-domain surrounding the disturbance, while the latter is aimed at representing the effect of the remaining of the system, for which the phasor approximation is good enough. Iterations are performed between the two simulations, each in charge of one sub-domain. This relaxation scheme is of the Gauss-Seidel type.

The method is expected to yield more accurate results than the fundamental-frequency model alone, while being significantly faster than an electromagnetic transients simulation performed over the whole system. Furthermore, some limitations of the fundamental-frequency approximation are removed, for instance in case of unbalanced fault analysis. To this purpose, and for accuracy, it may be necessary to increase the size of the sub-domain surrounding the disturbance.

Compared to other techniques presented in the literature, the proposed method does not require to identify and include in the electromagnetic transients simulation an equivalent of the sub-domain covered by fundamental-frequency simulation.

The interface variables between both simulations consist of voltages and currents at the boundary buses. Instantaneous sequence components were used to facilitate the extraction of the fundamental-frequency component of the currents injected at the interface.

Those features contribute to keeping the proposed hybrid simulation relatively simple.

Illustrative, preliminary simulation results have been shown on a small system but in demanding test cases. A comparison with a full EMTP-RV simulation of the whole system has been provided.

The next steps of the research will involve tests on a larger detailed sub-domain, while attention will be paid to accelerating the convergence of the relaxation procedure.

References

[1] V. Jalili-Marandi, V. Dinavahi, K. Strunz, J. Martinez, and A. Ramirez, "Interfacing techniques for transient stability and electromagnetic transient programs," *IEEE Transactions on Power Delivery*, vol. 24, no. 4, pp. 2385 – 2395, 2009.

[2] T. Demiray, G. Andersson, and L. Busarello, "Evaluation study for the simulation of power system transients using dynamic phasor models," in *Proceedings of Transmission and Distribution Conference and Exposition: Latin America, IEEE/PES*, Aug. 13-15 2008.

[3] K. Strunz, R. Shintaku, and F. Gao, "Frequency-adaptive network modeling for integrative simulation of natural and envelope waveforms in power systems and circuits," *IEEE Transactions on Circuits and Systems I: Regular Papers*, vol. 53, no. 12, pp. 2788–2803, December 2006.

[4] S. Fan and H. Ding, "Time domain transformation method for accelerating emtp simulation of power system dynamics," *IEEE Transactions on Power Systems*, vol. 27, no. 4, pp. 1778 –1787, nov. 2012.

[5] M. Heffernan, K. Turner, J. Arrillaga, and C. Arnold, "Computation of ac-dc system disturbances - part i. interactive coordination of generator and converter transient models," *IEEE Transactions on Power Apparatus and Systems*, vol. 100, no. 11, pp. 4341 – 4348, 1981.

[6] K. Turner, M. Heffernan, J. Arrillaga, and C. Arnold, "Computation of ac-dc system disturbances - part ii. derivation of power frequency variables from converter transient response- part iii. transient stability assessment," *IEEE Transactions on Power Apparatus and Systems*, vol. 100, no. 11, pp. 4349 – 4363, 1981.

[7] W. zhuo Liu, J. xian Hou, Y. Tang, L. Wan, X. li Song, and S. tao Fan, "An electromechanical/electromagnetic transient hybrid simulation method that considers asymmetric faults in an electromechanical network," in *Proceedings of the Power Systems conference and exposition (PSCE)*, Phoenix, USA, March 20-23 2011.

[8] A. van der Meer, R. Hendriks, M. Gibescu, and W. Kling, "Interfacing methods for combined stability and electro-magnetic transient simulations applied to vsc-hvdc," in *Proceedings of International Conference on Power System Transients (IPST)*, Delft, The Netherlands, 2011.

[9] S. Abhyankar and A. Flueck, "An implicitly-coupled solution approach for combined electromechanical and electromagnetic transients simulation," in *Power and Energy Society General Meeting, 2012 IEEE*, july 2012, pp. 1 –8.

[10] M. La Scala, M. Brucoli, F. Torelli, and M. Trovato, "A Gauss-Jacobi-Block-Newton method for parallel transient stability analysis (of power systems)," *IEEE Transactions on Power Systems*, vol. 5, no. 4, pp. 1168–1177, 1990. [Online]. Available: http://ieeexplore.ieee.org/lpdocs/epic03/wrapper.htm?arnumber=99367

[11] J. Reeve and R. Adapa, "A new approach to dynamic analysis of ac networks incorporating detailed modeling of dc systems. part i: principles and implementation," *IEEE Transactions on Power Delivery*, vol. 3, no. 4, pp. 2005 – 2011, 1988.

[12] S.-K. Chung, "A phase tracking system for three phase utility interface inverters," *IEEE Transactions on Power Electronics*, vol. 15, no. 3, pp. 431 –438, may 2000.

[13] G. Paap, "Symmetrical components in the time domain and their application to power network calculations," *IEEE Transactions on Power Systems*, vol. 15, no. 2, pp. 522 –528, may 2000.

[14] T. Van Cutsem, "Description, modeling and simulation results of a test system for voltage stability analysis," University of Liège, Internal report, 2013. [Online]. Available: http://hdl.handle.net/2268/141234

[15] D. Fabozzi, B. Haut, A. Chieh, and T. Van Cutsem, "Accelerated and localized newton schemes for faster dynamic simulation of large power systems," *to appear in IEEE Transactions on Power Systems (2013 Special section on Analysis and Simulation of Very Large Power Systems)*. [Online]. Available: http://hdl.handle.net/2268/141234